

## $V_s$ DETERMINATION FROM STEADY STATE RAYLEIGH WAVE METHOD

KOHJI TOKIMATSU<sup>1)</sup>, SHINICHI KUWAYAMA<sup>11)</sup>, SHUJI TAMURA<sup>111)</sup>  
and YASUO MIYADERA<sup>111)</sup>

### ABSTRACT

An improved version of steady state Rayleigh wave method is presented for the determination of shear wave velocity ( $V_s$ ) profiles of a horizontally stratified soil deposit. A dispersion curve and particle orbits of Rayleigh waves can readily be determined in the field through measurements of ground motions induced by an exciter using sensors placed on the ground surface. To determine  $V_s$ -profile from the dispersion curve, an inverse analysis which can take into account higher modes of Rayleigh waves is presented and used. To increase the effectiveness of the proposed method, desirable distances among the exciter and sensors are indicated, and the measured particle orbits are used to validate the inverted  $V_s$ -profile. Comparative field tests are made at two sites using the proposed method and the conventional down hole method. The  $V_s$ -profiles from the two methods are in good agreement with each other, indicating the effectiveness of the proposed method.

**Key words:** field test, geophysical exploration, inverse analysis, Rayleigh wave, shear wave velocity, surface wave, vibration, wave propagation (IGC: C2/D7/E8)

### INTRODUCTION

Shear wave velocity is an important soil property for the evaluation of dynamic behavior of soils as well as static deformation of the ground. Most of the field tests currently conducted for determining  $V_s$ -profiles require boreholes, and thus are costly and may not conveniently be used in all cases.

The determination of  $V_s$ -profiles from Rayleigh wave methods is promising and attractive,

since the field measurements can be performed just by placing sensors on the ground surface and without any boreholes. Besides, the method has a potential capability to detect a relatively soft layer sandwiched by stiffer layers, which capability cannot be offered by any other investigation made on the ground surface.

Such simple and yet efficient site investigation is particularly preferable for Seismic Microzonation such as the evaluation of safety of each house in a large area and the identifi-

<sup>1)</sup> Associate Professor, Tokyo Institute of Technology 2-12-1 O-okayama, Meguro-ku, Tokyo 152.

<sup>11)</sup> Research Student, ditto; and Research Engineer, Takechi Engineering Co. LTD.

<sup>111)</sup> Graduate Student, Tokyo Institute of Technology.

Manuscript was received for review on June 26, 1990.

Written discussions on this paper should be submitted before January 1, 1992, to the Japanese Society of Soil Mechanics and Foundation Engineering, Sugayama Bldg. 4F, Kanda Awaji-cho 2-23, Chiyoda-ku, Tokyo 101, Japan. Upon request the closing date may be extended one month.

cation of weak spots along lifeline facilities. It may also be desirable for preliminary field investigation to be conducted prior to more detailed site investigation, and for quality control of ground improvement.

To determine  $V_s$ -profiles, the Rayleigh wave method requires both the measurements of the relationship between phase velocity and wavelength, called dispersion curve, and the inverse analysis on the measured curve. Although several methods have been proposed and have demonstrated their potential, they have shown limitations in many aspects and thus not yet been used routinely and reliably.

The objects of the paper are to develop a computer-controlled system to measure Rayleigh wave dispersion curves, and to discuss requirements concerning field measurements and in-house analyses for a reliable determination of  $V_s$ -profiles.

## REVIEW OF PREVIOUS STUDIES

The possible determination of  $V_s$ -profiles of sub-surface soils based on the Rayleigh wave method has been studied by many investigators (e. g., Jones, 1958; Heukelon and Foster, 1960; Abbiss, 1981; and Stokoe et al., 1984). The procedure adopted in most of these methods involves:

(1) the generation of predominant vertical ground motions using an artificially induced point source, (2) the determination of dispersion curves, based on the measurements of ground surface motions using sensors placed in a line with the origin of the source, and (3) the determination of  $V_s$ -profiles based on the analysis on the measured dispersion curve.

The principle of these methods lies in the following facts:

(1) Two thirds of the total energy from a vertical point source goes to Rayleigh waves (Miller and Pursey, 1955), though other surface wave and body waves are also generated. Besides the attenuation of surface waves with distance from a point source is much smaller than that of body waves, i. e., the surface waves attenuate with a square root of distance, while the body waves attenuate with a square

of distance along the surface (Woods, 1968). Thus, the ground motions enough away from a point source are considered predominant Rayleigh waves.

(2) The phase velocity of the Rayleigh wave varies depending on wavelength or frequency. The waves with short wavelengths or high frequencies sample soil properties at small depth, whereas the waves with large wavelengths or low frequencies reflect properties of soil from the ground surface to much larger depth. In this respect, the Rayleigh wave is dispersive, and thus the correlation between phase velocity and wavelength or frequency is called dispersion curve. The inverse analysis of the curve can result in  $V_s$ -profiles of sub-surface soils, on the condition that the soil layer is horizontally stratified.

Concerning field observation of Rayleigh waves, Jones (1958) was probably the first to introduce the method into the field of geotechnical engineering. He used an exciter to induce vertical ground motions, and succeeded in constructing a dispersion curve. Since the frequency generated by the exciter ranged above 35 Hz, the dispersion curve was determined only for wavelengths shorter than 5 m. This provides  $V_s$ -profiles to the depth of only few meters. Heukelon and Foster (1960) and Abbiss (1981) also conducted Rayleigh wave measurements using improved apparatus and procedure, but were faced with similar problems when exploring deeper soil properties.

Unlike previous studies, Stokoe et al. (1984) used impulsive point sources to generate and measure Rayleigh waves and determine a dispersion curve through spectrum analysis on the observed motions. Since random vibrations were used in place of sinusoidal vibrations, its result may become inaccurate in the frequency ranges for which signal-to-noise (SN) ratio is low. This poses a problem in determining  $V_s$ -profiles at large depths (deeper than 10 m), since it is difficult, if not impossible, to generate low frequency waves with high SN ratios.

For the determination of  $V_s$ -profiles in the aforementioned procedures except one by Stokoe et al. (1984), it was assumed that the Rayleigh wave represents the property of soils

from the ground surface to a depth of a half of its wavelength. This assumption is empirical and lacks rigorous theoretical background. Thus the analysis based on  $1/2$  wavelength cannot provide reliable  $V_s$ -profiles in all cases. For example, it yields higher shear wave velocities than would be the case if a stiff layer exists near the ground surface (Stokoe et al., 1984). Further, it cannot automatically identify the boundary between layers with different properties. Accordingly, soil layering must be determined based on experience or other information.

Besides, all the methods completely lack the information to confirm whether the measured waves are Rayleigh waves and which mode of Rayleigh waves is actually dominant. Thus these limitations significantly lessen the accuracy of the resulting  $V_s$ -profiles from currently available Rayleigh wave methods, and require further studies toward improving the reliability of both the test procedure and the inverse analysis.

## DETERMINATION OF RAYLEIGH WAVE DISPERSION CURVE

### *Test Apparatus*

A test system is devised for the determination of Rayleigh wave dispersion curves

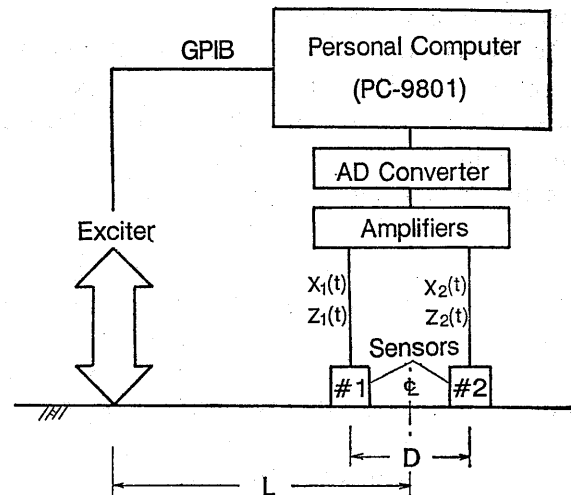


Fig. 1. Schematic diagram of test system

with sufficient degree of reliability. The system consists of a vertical exciter, two pairs of sensors, amplifiers, and a personal-computer. The exciter has a maximum driving force of either 20 kgf or 250 kgf over the frequency range 5 Hz to 200 Hz. The sensors are velocity transducers with a natural frequency of 1 Hz, and have the maximum sensitivity of 3.4V/kine. The amplifiers have the maximum amplification factor of 2000. The personal computer is a model called PC9801VX produced from NEC, equipped with an AD converter and a GPIB interface. The AD converter has a resolution of 12 bits.

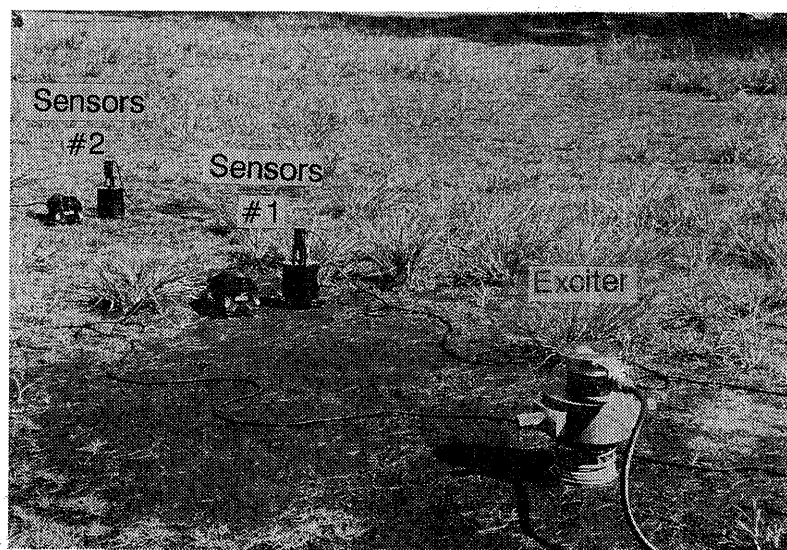


Photo. 1. Test arrangements

### Test Arrangements

As shown in Fig. 1, a point is selected on the ground surface (located on the center line) under which  $V_s$ -profile is to be determined. The exciter is placed on the ground surface at a horizontal distance of  $L$  from the point. In the line with the exciter and the point, two pairs of sensors, designated as #1 and #2, are placed symmetrically about the center line with a distance of  $D$ . Each pair of sensors can measure vertical and radial ground surface motions induced by the exciter. As explained later, this arrangement can yield the phase velocity and particle orbits of Rayleigh waves traveling along the ground surface. The outline of the test setup is shown in Photo 1.

It is known that the particle orbit of Rayleigh waves in any place in the ground is elliptical in the vertical plane containing the direction of propagation of the wave, as shown in Fig. 2. In an ideal case, the horizontal particle motion is either behind or ahead the vertical one 90 degree in phase. This means that the orbit is either prograde elliptical or retrograde elliptical and that the major and minor axes of the ellipse correspond to the vertical and horizontal axes.

These characteristics of particle orbits may vary depending on the mode and wavelength of Rayleigh wave as well as the soil profile underground. Thus such information may be used to identify which mode of Rayleigh wave is predominant and whether or not the measured motions are Rayleigh waves. This is the reason that the radial motions are measured in conjunction with the vertical motions, which measurements have been missing in any previous study.

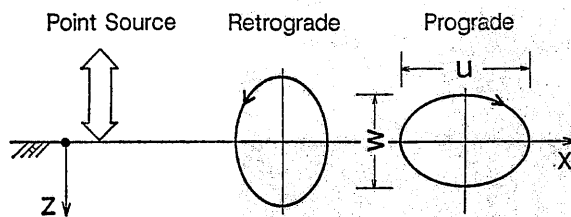


Fig. 2. Particle orbits of the Rayleigh wave

### Test Procedure and Field Analysis

The exciter oscillates with a simple vertical harmonic motion, of which frequency,  $f_i$ , and amplitude are controlled by the computer through the GPIB interface (Fig. 1). The analog motions measured with the sensors are amplified and then converted into a digitized form by the AD-converter. The digitized motions in the time domain are defined as  $z_1(t)$ ,  $z_2(t)$ ,  $x_1(t)$ , and  $x_2(t)$  in which  $z$  and  $x$  indicate vertical and horizontal motions, and the subscripts 1 and 2 correspond to sensor number. The AD-conversion and the following spectrum analysis are usually made for 2048 or 4096 digitized points at equal time intervals.

On completion of the AD conversion, the digitized motions are transformed from the time domain to the frequency domain,  $S_{z1}(f)$ ,  $S_{z2}(f)$ ,  $S_{x1}(f)$  and  $S_{x2}(f)$ , by the Fast Fourier Transform. The cross power spectrum between the two digitized vertical motions is given by:

$$G_{z1z2}(f) = S_{z1}^*(f) S_{z2}(f) \quad (1)$$

in which  $*$  indicates the complex conjugate. The phase lag of the motions between the two observed points,  $\phi_i$ , at frequency  $f_i$  can be determined by:

$$\phi_i = -\tan^{-1}(Q_{z1z2}(f_i) / K_{z1z2}(f_i)) \quad (2)$$

in which  $K$ =real part of  $G$  and  $Q$ =imaginary part of  $G$ . In case that the amplitude of vertical motions is significantly less than that of horizontal motions, the computation of phase lag may be made using horizontal motions.

The time lag of motions between the two observed points,  $\Delta t$ , is then given by:

$$\Delta t = \phi_i / 2\pi f_i \quad (3)$$

The phase velocity,  $c_i$ , can be calculated from:

$$c_i = D / \Delta t \quad (4)$$

By noting  $c = f\lambda$ , the corresponding wavelength,  $\lambda$ , can readily be determined.

The particle orbit at each observed point can be obtained by plotting its horizontal and vertical motions on a  $x$ - $z$  plane. The amplitude ratio between horizontal and vertical motions,  $u/w$ , (see Fig. 2) may be given by:

$$(u/w)_{in} = \text{sign}[Q_{xz}(f_i)] \frac{|S_{xn}(f_i)|}{|S_{zn}(f_i)|} \quad (5)$$

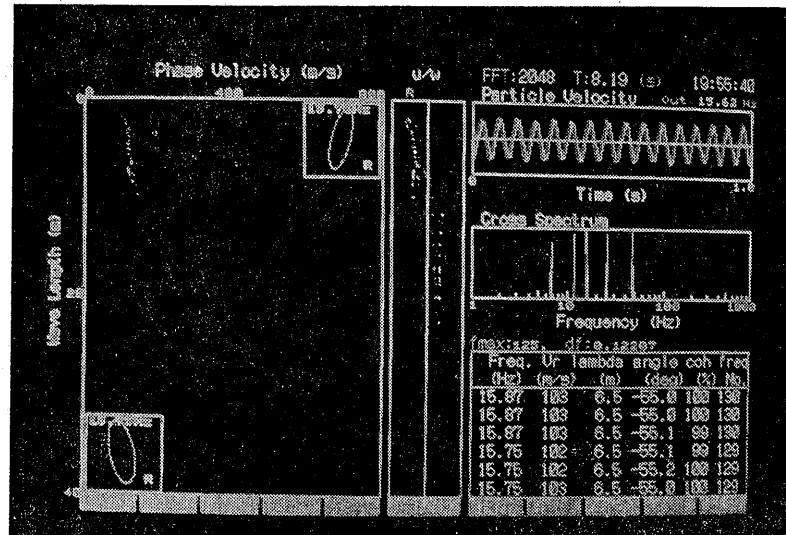


Photo. 2. CRT display of personal computer during test

in which  $n$  indicates sensor number. Positive values of  $u/w$  indicate that the particle orbit is prograde, and negative values correspond to retrograde. Large absolute values mean that horizontal motions prevail, while small absolute values indicate dominance of vertical motions.

The phase velocity, the particle orbits, and the amplitude ratios thus determined can readily be displayed in the CRT of the computer such as shown in Photo 2, and stored with the raw recorded motions in a disk for in-house analyses.

The aforementioned measurements and analyses are repeated by changing frequency of the exciter. Owing to the good performance of the computer, the measurements and analyses can be conducted in almost real time. It takes about a half hour to measure a dispersion curve with a maximum wavelength of 50 m, which could provide  $V_s$ -profiles to a depth of about 20 m.

### REQUIRED DISTANCES AMONG EXCITER AND SENSORS

In order to determine suitable distances among the exciter and the sensors, a series of special tests was made in which additional sensors were set in the ground, as shown in Fig. 3. Dispersion curves were measured for  $L=1.5$ ,

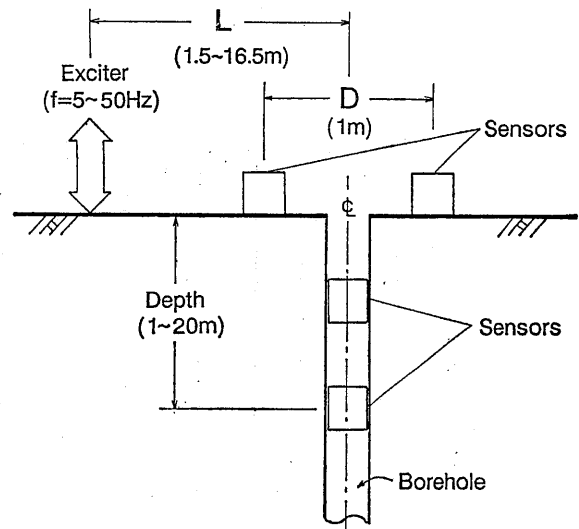


Fig. 3. Schematic cross section of test arrangement

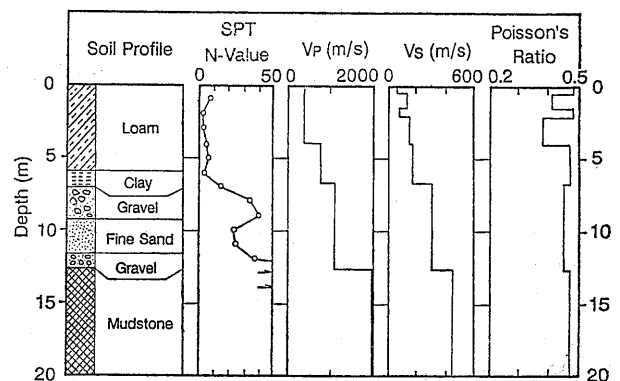


Fig. 4. Geological and geophysical logs

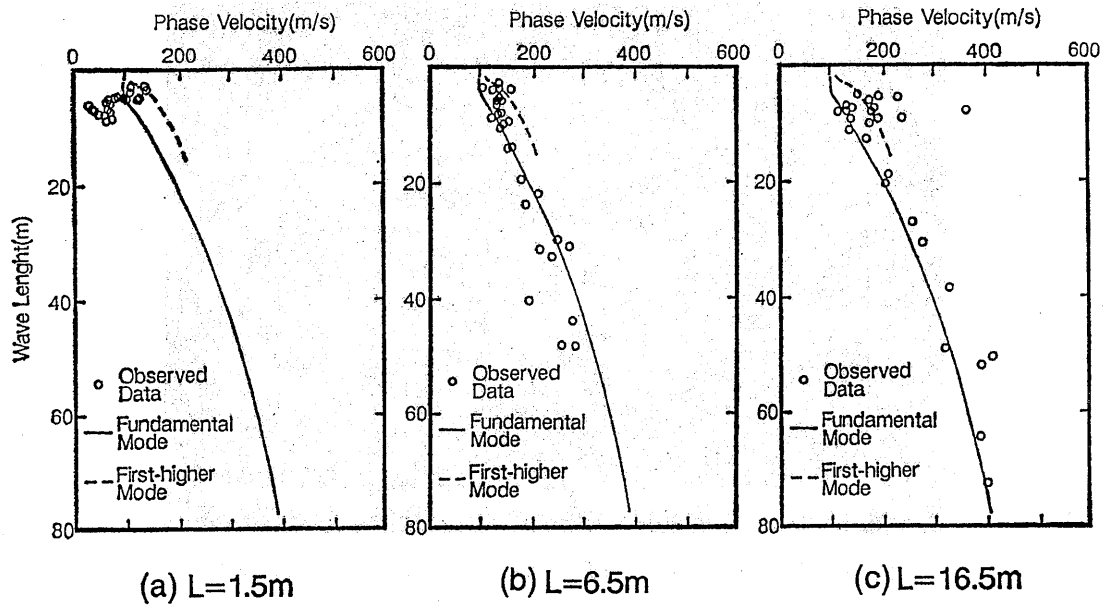


Fig. 5. Observed and computed correlation between phase velocity and wavelength

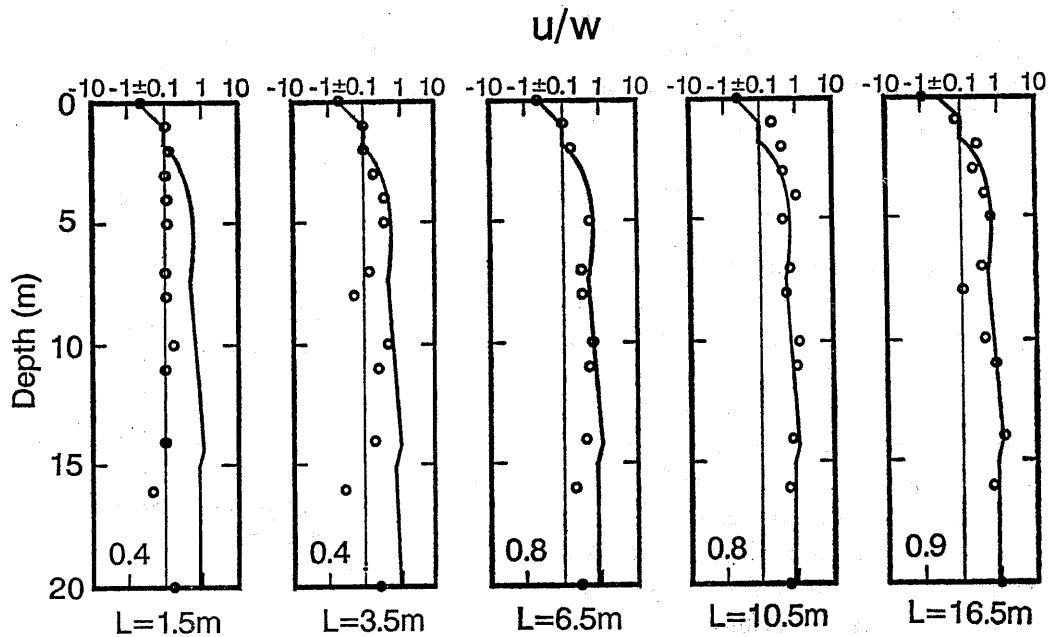


Fig. 6. Observed and computed  $u/w$  with depth at  $f=10$  Hz

3.5, 6.5, 10.5, and 16.5 m, and the corresponding particle orbits were determined at depths from 0 to 20 m for each  $L$ , with  $D=1$  m.

The geological and geophysical logs of the test site determined from the standard penetration test and down hole method are shown in Fig. 4. The layer between 0 m to 6 m consists of loam and clay. It is relatively soft,

with SPT  $N$ -values less than 3 and with most values of shear wave velocity,  $V_s=150$  m/s. It is underlain by 6 m-thick cohesionless soils with a shear wave velocity of about 300 m/s. The layer below 12 m is stiff mudstone with  $V_s$  more than 400 m/s.

Fig. 5 shows the observed correlation between phase velocity and wavelength for  $L=$

1.5, 6.5 and 16.5 m, using open symbols. Also shown in the figure are the fundamental and first higher modes of dispersion curves computed from theory (Haskell, 1953) using the  $V_s$  profile shown in Fig. 4.

It seems that the phase velocities with large wavelengths are determined better for large  $L$  than for short  $L$ . This is probably due to the short distance of  $L$  compared with the measured wavelength. With a point source nearby, the measured particle motions may not directly correspond to those given by the Haskell's theory because of the following reasons: (1) presence of body wave, and (2) the Haskell's theory assumes two dimensional plane waves, whereas the actual problem is axisymmetric.

The phase velocities with short wavelengths, in contrast, show considerable variation at large  $L$ . The cause of this is unknown, but partly referred to the coexistence of several higher modes that tend to dominate with distance from the source at short wavelength.

The above discussions indicate that there exists an appropriate distance among exciter and sensors if a reasonable result is to be obtained and that the required distance depends on wavelength measured. Tanaka et al. (1989) have presented the same conclusion based on similar investigation conducted at the other site.

To determine possible requirements for the distance, the amplitude ratios of the particle orbits at  $f=10$  Hz measured at various depths in the borehole and at various distances from the exciter are plotted on a semi-log scale in Fig. 6 in open symbols. Note that vertical motions appear to dominate near the exciter throughout the depths, contradicting the general behavior of Rayleigh waves.

For comparison purposes, the amplitude ratios with depth were computed from theory (Haskell, 1953) for the measured  $V_s$ -profile shown in Fig. 4 and are shown in Fig. 6 using solid curves. As expected, discrepancy from the theory is evident for the observation made near the exciter. The correlation coefficients between the observed and theoretical values are computed and indicated in the lower corner

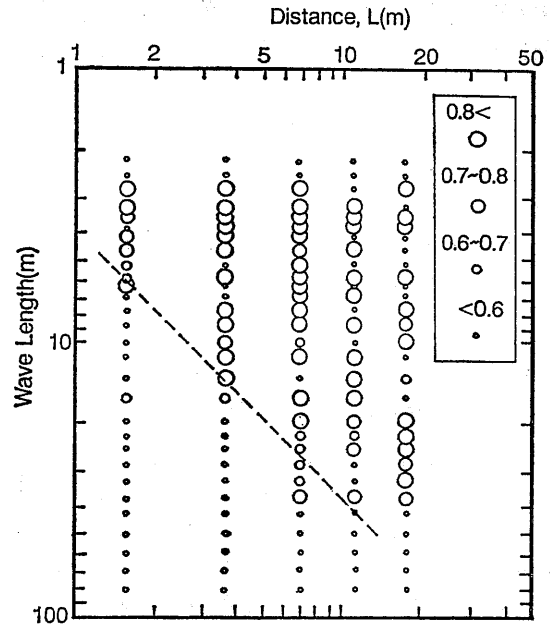


Fig. 7. Correlation coefficient between observed and computed  $u/w$  in terms of wavelength and distance from exciter

of the figure. It seems that the greater the distance between the exciter and the sensors, the better becomes the agreement between theory and observation.

Similar analyses were made for different frequencies, and results are summarized in Fig. 7 in which correlation coefficients between theory and observation are shown in terms of distance,  $L$ , and wavelength. It seems that a high correlation coefficient is generally expected above the broken line, i. e.,  $L$  is more than a quarter of wavelength. This confirms that the distance of  $L$  should be increased with increasing wavelength if a reasonable result is to be obtained.

To maintain the accuracy and reliability of phase velocity computed from Eq. (4) throughout the test,  $\Delta t$  should not be too small, which requires that  $D$  should be also increased with increasing wavelength. Moderate variation in the observed data at large wavelengths shown in Fig. 5(c) is probably due to the use of a small value of  $D$  compared with large wavelengths.

Based on the above discussions and several experiences, the following empirical rules are

tentatively set for the following field investigation.

$$\lambda/4 \leq L \quad (6)$$

$$\lambda/16 \leq D < \lambda \quad (7)$$

Generally, two or three different arrangements in terms of distances  $L$  and  $D$  are sufficient for the determination of  $V_s$ -profiles to a depth of about 20 m.

### DETERMINATION OF $V_s$ -PROFILES FROM DISPERSION CURVE

Haskell (1953) developed a theory for determining phase velocity vs. wavelength relationship of the fundamental and higher modes of Rayleigh waves for a horizontally stratified soil deposit consisting of  $N$  layers as shown in Fig. 8. Each layer is homogeneous and isotropic, and is characterized by thickness,  $H$ , mass density,  $\rho$ ,  $P$ -wave velocity,  $V_p$ , and  $S$ -wave velocity,  $V_s$ . Since the theory does not provide information concerning the degree of participation of each mode, its direct use in the inverse analysis is limited to the case where only the fundamental mode dominates.

Harkrider (1964) extended the theory to an axisymmetric problem with a point source, and determined the degree of participation of each mode, called medium response factor. Combining with these studies to take into account the effects of both the fundamental and higher modes, the phase velocity and the amplitude ratio to be observed on the ground surface for a given frequency,  $f_i$ , can be expressed by:

Layer No.	Thickness	Density	P-Wave Velocity	S-Wave Velocity
1	$H_1$	$\rho_1$	$V_{p1}$	$V_{s1}$
2	$H_2$	$\rho_2$	$V_{p2}$	$V_{s2}$
$\vdots$	$\vdots$	$\vdots$	$\vdots$	$\vdots$
$N-1$	$H_{N-1}$	$\rho_{N-1}$	$V_{pN-1}$	$V_{sN-1}$
$N$	$\infty$	$\rho_N$	$V_{pN}$	$V_{sN}$

Fig. 8. One-dimensional model

$$c_i = F(f_i, L: a_1, a_2 \cdots a_J) \quad (8)$$

$$(u/w)_i = G(f_i, L: a_1, a_2 \cdots a_J) \quad (9)$$

in which each  $a$ -value corresponds to one of the soil properties of a layer as shown in Fig. 8. Since  $N$ th layer is a halfspace, the total number of  $a$ -values to be needed,  $J$ , is  $4N-1$ .

The determination of  $V_s$ -profiles from measured Rayleigh wave dispersion curves requires an inverse analysis of Eq. (8). If the phase velocities,  $c_{ei}$ , are measured for  $I$  different frequencies,  $f_i$ , from field observation, the inversion is to find soil properties that minimize the following:

$$S = \sum_{i=1}^I (c_{ei} - c_i)^2 \quad (10)$$

in which  $c_i$  is given by Eq. (8). Eq. (10) can be solved using a modified version of the nonlinear optimizing method originally proposed by Dorman and Ewing (1962) as follows under the condition that  $I \gg J$ :

Assuming appropriate values of soil properties as the first approximation and setting these values as elements of  $A$  vector, correction parameters of  $A$  vector,  $\Delta A$ , can be given by solving the following  $J$  simultaneous equations:

$$P^T P \Delta A = P^T C \quad (11)$$

in which  $T$  denotes the transpose of a matrix;  $P$  is a matrix with  $I$  rows and  $J$  columns, whose element is  $dc_i/da_j$ ;  $C$  is a column vector whose element is the difference between computed phase velocity and observed one, i. e.,  $c_{ei} - c_i$ .  $A$  is then updated by:

$$A = A + \mu \Delta A \quad (12)$$

in which  $\mu$  is a constant that makes  $S$  minimal.

Assuming modified  $A$  vector as new soil properties, the above computation is repeated until the least mean square,  $S$ , becomes practically zero, i. e., the computed dispersion curve matches with the observed one.

As is known, this type of inversion does not provide a unique solution without some constraints or other information. To overcome this defect, if not completely, inverse analyses were made assuming several initial models, and the comparison was made to check whether the computed particle orbits of each inverted model are consistent with the observed



ones. Finally, among the inverted models, one that is best consistent with both the observed dispersion curve and particle orbits is considered as the actual soil profile. With this comparison, the solution is considered almost unique from an engineering point of view.

Because the effect of the difference in density and  $P$ -wave velocity on the correlation between  $f_i$  and  $\alpha_i$  is negligibly small, the total number of layer properties to be determined in the inversion analysis can be reduced to  $2N-1$ . For a soil deposit for which thickness of each layer is known from other investigation, the total number of properties may be further reduced to  $N$ . However, solving inversion with  $2N-1$  unknown values provides a set of  $V_s$  values and layering which are completely independent of any other geological and geophysical investigation.

#### COMPARISON OF SHEAR WAVE VELOCITY PROFILES FROM RAYLEIGH WAVE METHOD WITH THOSE FROM DOWN HOLE METHOD

In order to evaluate the effectiveness of the proposed method, comparative field tests were made at two sites in Niigata city, called Sites A and B. The field tests included the Rayleigh wave method, the conventional downhole seismic propagation tests, and the SPT tests. The geological and geophysical logs of the sites determined from the conventional method are shown in Figs. 9 and 10. At Site A, the

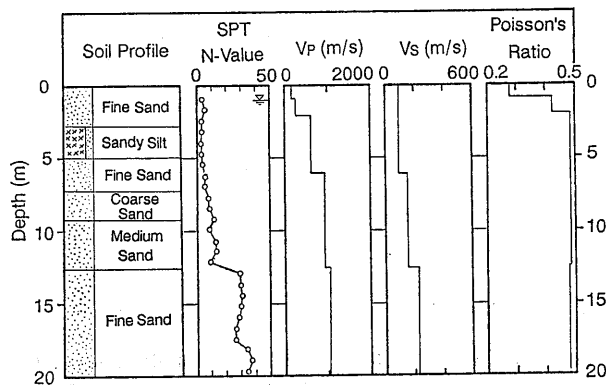


Fig. 9. Geological and geophysical logs for Site A

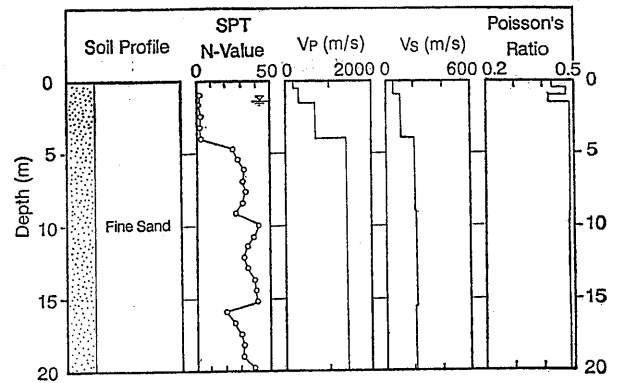


Fig. 10. Geological and geophysical logs for Site B

layer from ground surface to a depth of about 6 m is very loose sand with  $N$ -values generally less than 5 which is underlain by medium dense sand, and the layer below 12.5 m is dense sand. At Site B, in contrast, a layer of dense sand is overlain by a thin loose sand layer.

Figs. 11 and 12 show the results of the proposed Rayleigh wave investigation in which measured wavelength is plotted against (a) phase velocity and (b)  $u/w$ , in open circles. Generally the longer the wavelength the larger becomes the phase velocity as shown in Figs. 11 (a) and 12 (a) for wavelengths longer than

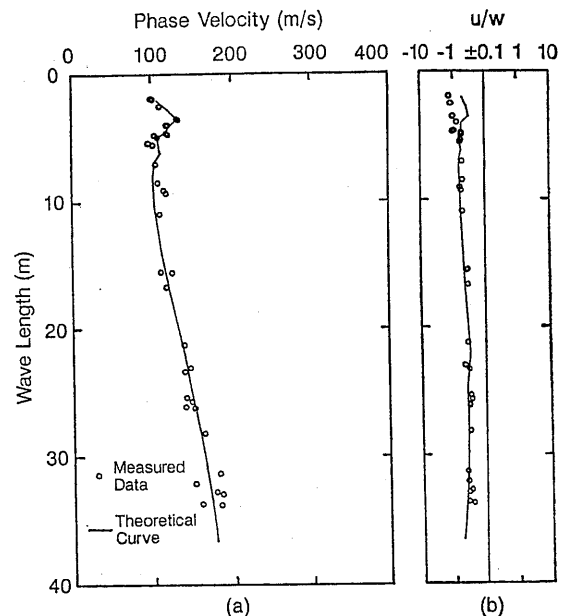


Fig. 11. Observed and computed dispersion curves and  $u/w$  for Site A

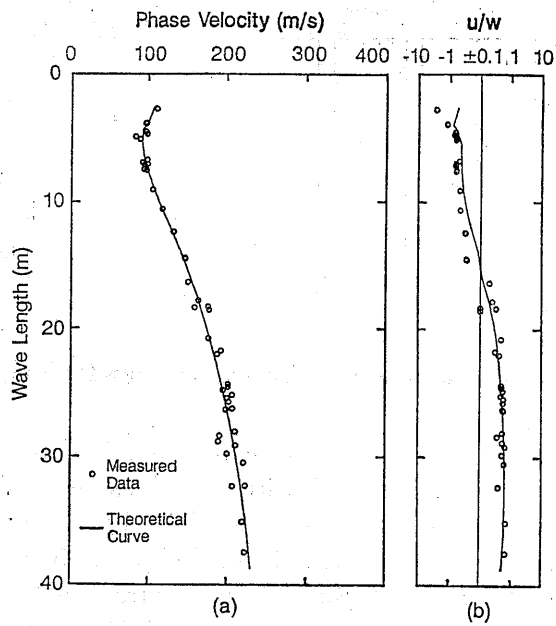


Fig. 12. Observed and computed dispersion curves and  $u/w$  for Site B

5 m. In this wavelength range, the Rayleigh wave is considered to be normally dispersive in which the fundamental mode is generally dominant. However, the trend reverses for shorter wavelengths, probably reflecting higher modes of Rayleigh waves. It is known that the presence of stiff layer near the ground surface tends to induce higher modes of Rayleigh waves, which is considered to be the main cause of the above mentioned trend.

The particle orbit at Site A in Fig. 11(b) is retrograde for any wavelengths, whereas it is retrograde for wavelengths less than 20 m and prograde thereafter at Site B as shown in Fig. 12(b). The difference in the pattern of particle orbits probably reflects difference in the variation of soil stiffness with depth.

Inverse analysis was then performed with these data assuming a five to six layer model with appropriate initial soil properties. The solid lines in Figs. 11(a) and 12(a) are the resulting dispersion curves that best fit to the

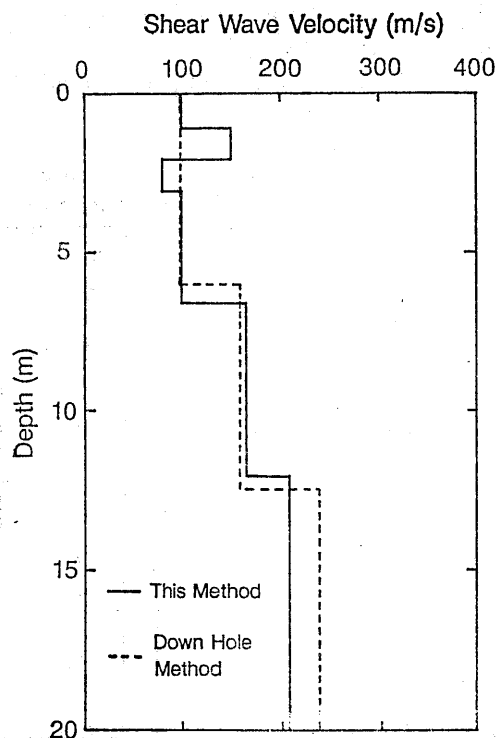


Fig. 13. Comparison of  $V_s$  profiles determined by the proposed Rayleigh wave method and downhole method at Site A

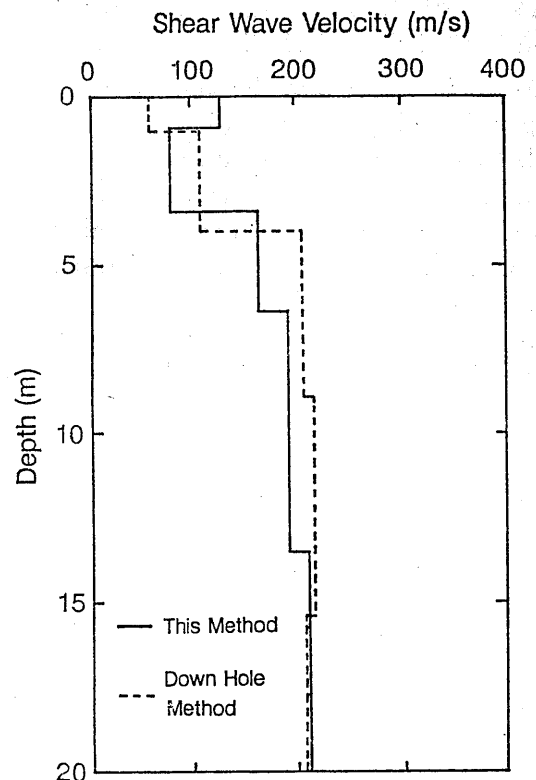


Fig. 14. Comparison of  $V_s$  profiles determined by the proposed Rayleigh wave method and downhole method at Site B

measured values. The solid lines in Figs. 11(b) and 12(b) are the variations of amplitude ratio with wavelength computed from Eq. (9) for the inverted  $V_s$ -profiles. The good agreements in both phase velocity and  $u/w$  between the observed and computed values indicate that the inversion is successfully conducted. Particularly noted is the good simulation in trend of the computed dispersion curve at short wavelengths shown in Figs. 11(a) and 12(a). This cannot be obtained without considering the effect of higher modes in the inversion.

The solid lines in Figs. 13 and 14 are the corresponding  $V_s$ -profiles. For comparison,  $V_s$ -profiles from the conventional down hole method are shown in the figure. Good agreements in  $V_s$ -profiles suggest that the proposed method and analysis are effective. The figure also indicates that the Rayleigh wave investigation can result in  $V_s$ -profiles as reliably as the conventional method to depths less than at least about one third of the maximum wavelength measured.

## CONCLUSIONS

An improved version of measuring system and inverse analysis of steady state Rayleigh wave method has been developed for a better determination of  $V_s$ -profiles. This has been accomplished by: (1) the measurements of particle orbits in a vertical plane, (2) the selection of appropriate distances among the exciter and sensors, (3) the consideration of the effects of higher modes in the inverse analysis, and (4) the validation of the inverted model using measured particle orbits.

Comparative field tests indicated that the  $V_s$ -profiles and particle orbits from the proposed Rayleigh wave method are in good agreement with those obtained and computed from the downhole method, and that the proposed method is effective.

## ACKNOWLEDGMENTS

Financial support provided by the Ministry of Education, Science and Culture, is greatly appreciated.

## REFERENCES

- 1) Abbiss, C. P. (1981): "Shear wave measurements of the elasticity of the ground," *Géotechnique*, 31, No. 1, pp. 91-104.
- 2) Dorman, J. and Ewing, M. (1962): "Numerical inversion of seismic surface wave dispersion data and crust-mantle structure in the New York-Pennsylvania area," *Journal of Geophysical Research*, Vol. 67, No. 13, pp. 5227-5241.
- 3) Harkrider (1964): "Surface waves in multilayered elastic media I. Rayleigh and Love waves from buried sources in a multilayered elastic half-space," *Bulletin of the Seismological Society of America*, Vol. 54, No. 2, pp. 627-679.
- 4) Haskell, N. A. (1953): "The dispersion of surface waves on multilayered media," *Bulletin of Seismological Society of America*, Vol. 43, No. 1, pp. 17-34.
- 5) Heukelom, W. and Foster, C. R. (1960): "Dynamic testing of pavements," *Journal of the Structural Division, ASCE*, SM1, pp. 1-28.
- 6) Jones, R. B. (1958): "In-situ measurement of the dynamic properties of soil by vibration methods," *Geotechnique*, Vol. 8, No. 1, pp. 1-21.
- 7) Miller, G. F. and Pursey, H. (1955): "On the partition of energy between elastic waves in a semi-infinite solid," *Proceedings, Royal Society, London, Series A*, Vol. 233, pp. 55-69.
- 8) Stokoe, K. H. and Nazarian, S. (1984): "In situ shear wave velocity from spectral analysis of surface waves," *8th World Conference on Earthquake Engineering*, Vol. 3, pp. 31-38.
- 9) Tanaka, K., Tokimatsu, K., and Kuwayama, S. (1989): "System for evaluating  $V_s$  profiles based on Rayleigh wave method," *Proc., 24th Annual Meeting of JSSMFE*, Vol. 1, pp. 701-702, (in Japanese).
- 10) Woods, R. D. (1968): "Screening of surface waves in soils," *Journal of the Soil Mechanics and Foundations Division, ASCE*, Vol. 94, No. SM4, pp. 951-979.